

A survey of electron-deficient pentacenes as acceptors in polymer bulk heterojunction solar cells†

Ying Shu,^a Yee-Fun Lim,^b Zhong Li,^a Balaji Purushothaman,^a Rawad Hallani,^a Jo Eun Kim,^b Sean R. Parkin,^a George G. Malliaras^{*b} and John E. Anthony^{*a}

Received 12th August 2010, Accepted 13th October 2010

DOI: 10.1039/c0sc00433b

We have prepared, characterized and surveyed device performance for a series of electron deficient pentacenes for use as acceptors in polymer bulk heterojunction solar cells, using P3HT as the donor material. All of the materials reported here behaved as acceptors, and variations in the position and nature of the electron-withdrawing group on the pentacene core allowed tuning of device open-circuit voltage. Photocurrent was strongly correlated with the pentacene crystal packing motif; materials with 2D π -stacking interactions performed poorly compared with materials exhibiting 1D π -stacking interactions. The best pentacene acceptors gave repeatable device efficiency in excess of 1.2%, compared with 3.5% exhibited for PCBM-based devices.

Solar energy conversion using solution processed organic semiconductors has been a field of increasing interest, and the promise of low-cost energy generation from lightweight, flexible solar panels has led to rapid progress in device performance. Since the first polymer donor/(6,6)-phenyl C₆₁ butyric acid methyl ester (PCBM) acceptor bulk-heterojunction (BHJ) solar cell,¹ dramatic advances have been made in improving power conversion efficiency in these systems.² Most research in this field has emphasized the development of new donor polymers³ and on improvements in processing conditions to yield optimum morphologies for charge transport,⁴ recently leading to impressive power conversion efficiency (PCE) in polymer/fullerene devices approaching 8%.⁵ Due to the outstanding performance of fullerene-based materials, efforts to discover new acceptors for polymer BHJ organic photovoltaics (OPVs) have been comparatively limited.⁶ Although polymeric acceptors recently yielded efficiency up to 2.0% in all-polymer devices,⁷ small-molecule acceptors, essentially used as drop-in replacements for PCBM, have not yet reached even that level of performance. Acceptors based on chromophores such as perylene diimide,⁸ Vinazene,⁹ and diketopyrrolopyrrole^{10,11} derivatives yielded P3HT-based BHJ solar cells with power conversion efficiencies as high as 0.55%, 0.75% and 1.0%, respectively – few other materials have shown efficiencies greater than ~0.5%,¹¹ although some promising new results hint at new routes to improved performance.¹²

The ease with which pentacene-based small-molecule acceptors can be synthetically altered to improve charge transport and film morphology makes these compounds ideal candidates for

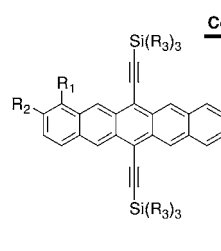
a systematic study of their structure-property relationships as OPV acceptors.¹³ We report here a survey of soluble pentacene derivatives with electron-withdrawing groups on the pentacene core, the impact of these groups on the open-circuit voltage of poly(3-hexylthiophene) (P3HT)/pentacene BHJ solar cells, and the optimization of top candidates to improve crystal packing and morphology. Several of the resulting materials yield photovoltaic cells with PCE greater than 1.0%, and the best performing derivative shows PCE approaching 1.3%.

In contrast with the degree of substitution required for electron transport in organic transistors,¹⁴ we recently found that only a single electron-withdrawing group – in that case a nitrile substituent – was necessary to achieve reasonable OPV performance with pentacene-based acceptors.¹⁵ For this study, we thus prepared a series of soluble pentacene derivatives with an array of electron-withdrawing groups on the pentacene core. Recent reports of the substituent positional sensitivity of electronic characteristics in pentacene derivatives¹⁶ led us to synthesize derivatives containing the electron-withdrawing group at both the 1- and 2-position on the acene ring (Fig. 1).

Results and discussion

Synthesis of the acceptors

The general synthesis of our pentacene acceptors is outlined in Schemes 1 and 2, and full synthetic details are provided in the ESI.† For most derivatives, the targets were accessed by addition



Compound	R ₁	R ₂	R ₃
1	H	CN	cyclopentyl
2	CN	H	iso-propyl
3	CF ₃	H	iso-propyl
4	H	CF ₃	iso-propyl
5	H	CF ₂ CF ₃	iso-propyl
6	NO ₂	H	iso-propyl
7	NO ₂	CCSi-Pr ₃	iso-propyl
8	H	NO ₂	iso-propyl
9	H	COOMe	iso-propyl
10	H	Cl	iso-propyl
11	H	H	iso-propyl

Fig. 1 Initial pentacene targets prepared for this study.

^aDepartment of Chemistry, University of Kentucky, Lexington, KY, 40506, USA. E-mail: anthony@uky.edu; Fax: +1 859 323 1069; Tel: +1 859 257 8844

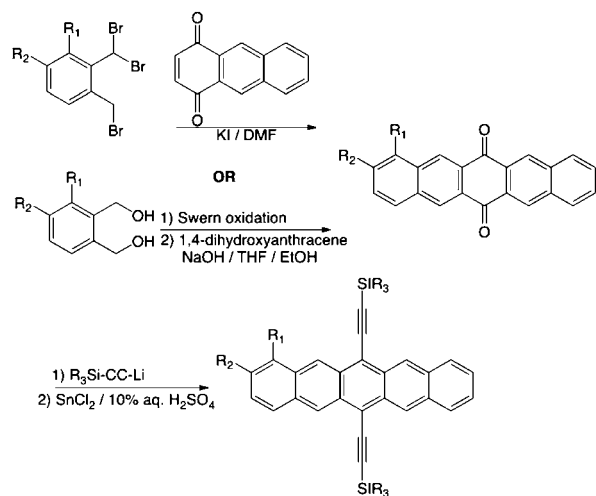
^bDepartment of Materials Science and Engineering, Cornell University, Ithaca, NY, 14850, USA. E-mail: ggm1@cornell.edu; Fax: +1 607 255 2365; Tel: +1 607 255 1956

† Electronic supplementary information (ESI) available: Synthesis and characterization of compounds 1–16, and details of device fabrication. CCDC reference numbers 796836–796840. For ESI and crystallographic data in CIF or other electronic format see DOI: 10.1039/c0sc00433b

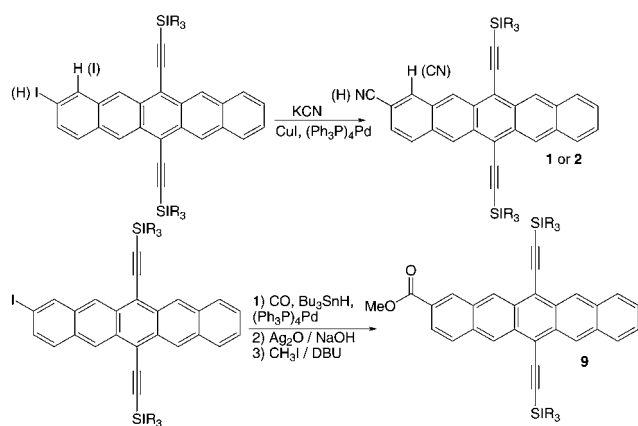
of a lithium acetylide to a pentacenequinone, followed by deoxygenation with SnCl_2 . Quinones were prepared by either aldol condensation or Cava reaction (Scheme 1). For the cyanopentacenes and carboxymethyl derivatives, the corresponding iodopentacenes were first prepared as outlined in Scheme 1, followed by Pd-mediated coupling of the desired functional group onto the pentacene core (Scheme 2). The only di-substituted derivative presented in this study (**7**) was formed as a major byproduct during the synthesis of compound **6**.

Characterization of the acceptors

Electrochemical analysis of these pentacene derivatives showed that they all possess LUMO levels appropriate to serve as acceptors for a P3HT-based donor (Table 1). As expected, the strongly electron-withdrawing nitro substituent yielded the lowest lying LUMO level of the materials tested in this study, followed by nitrile and perfluoroalkyl substituents. We noted only small differences in the LUMO energies between pentacenes substituted on the 1-position *versus* those substituted on the 2-position with the same functional group. These pentacene



Scheme 1 General synthetic approach to electron-deficient pentacenes (for R_1 or $R_2 = \text{CF}_3, \text{Cl}, \text{I}, \text{CF}_2\text{CF}_3, \text{NO}_2$).



Scheme 2 Synthesis of cyanopentacenes **1** and **2**, and carboxymethyl pentacene derivative **9**.

Table 1 Electrochemical^a data for electron-deficient pentacenes

Compound	HOMO/eV	LUMO/eV	Optical Gap/eV
PCBM	-6.10	-3.70	
1	-5.29	-3.50	1.82
2	-5.34	-3.50	1.81
3	-5.28	-3.41	1.86
4	-5.29	-3.45	1.83
5	-5.32	-3.42	1.86
6	-5.34	-3.52	1.73
7	-5.35	-3.61	1.78
8	-5.34	-3.55	1.73
9	-5.26	-3.49	1.80
10	-5.17	-3.33	1.85

^a Differential pulse voltammetry performed at a scan rate of 20 mV s^{-1} with Fc/Fc^+ as internal standard. Fc/Fc^+ is assumed to have an absolute energy level of -4.8 to vacuum.¹⁷ Optical gap calculated from the onset of absorption in dichloromethane solution.

derivatives all have similar optical absorption properties. The UV-vis spectra for typical pentacene acceptors (**1**, **4** and **10**), along with the spectrum for PCBM, are shown in Fig. 2. The acenes absorb with good intensity in the lower energy part of the visible spectrum, which may prove useful in extending the active window of OPV devices made from larger band gap polymers such as P3HT.

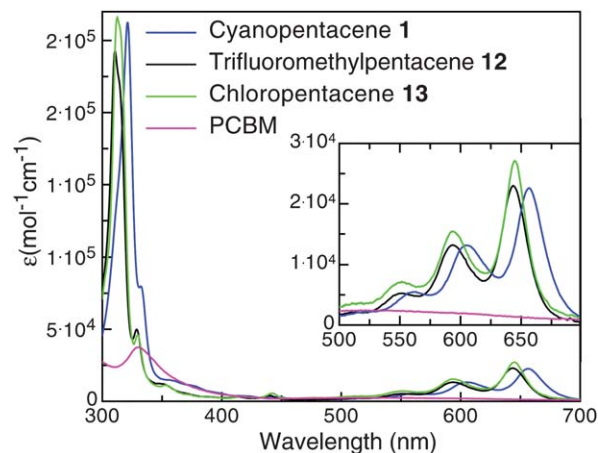


Fig. 2 Absorption spectra of representative pentacenes and PCBM.

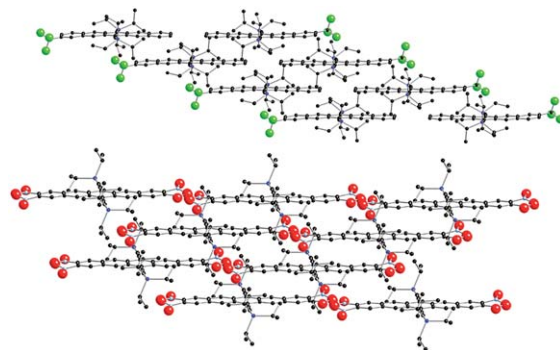


Fig. 3 Representative crystal packings. Top: double 1-D slipped-stack motif (**4**). Bottom: 2-D brickwork motif (**8**).

Several of the pentacene acceptors yielded solution-grown single crystals of sufficient quality for at least cursory structural analysis, as described in the ESI.† Consistent with this functionalization methodology, all of the materials adopted some form of π -stacked arrangement in the solid state.¹⁸ Among these derivatives, the most common motif was a double 1-D “slipped-stack” arrangement (Fig. 3, top), adopted by **4**, **5** and **7**. This motif is driven by the unsymmetrical substitution pattern in these materials, leading to the un-substituted ends of the acenes residing in close proximity in the crystal. The resulting pairwise-stacked acenes are insulated from adjacent stacks by the hydrocarbon substituents of those stacks. Nitro derivative **8** adopted a 2-D “brickwork” packing similar to that of TIPS pentacene **11**.¹⁹ The 1-substituted compounds (**2**, **3**, **6**) formed smaller crystals than the corresponding 2-substituted derivatives, that were too small for crystallographic analysis.

It is possible that the crystalline form of the material present in the P3HT blend is different from the single crystal form – analysis of the crystallites in the blend is currently underway.

Device optimization

Because cyano derivative **1** had already exhibited some level of performance as an OPV acceptor, the test procedure for these new materials was optimized using this compound. In our previous study, we defaulted to toluene as the solvent for spin-coating blends of P3HT and **1**.¹⁵ We observed that under these conditions, this pentacene derivative formed large micron-size crystals in the blend films. Since the exciton diffusion length in organic semiconductors is on the order of ~ 10 nm, the donor-acceptor domains need to be of that length scale for optimum solar cell performance.²⁰ Hence, for this study we attempted to suppress pentacene crystallization during film formation by the use of a process additive. The use of high-boiling additives such as alkanedithiols has been studied in the fabrication of traditional polymer/PCBM solar cells, and dramatically improved the performance of the resulting devices.^{3c,4a,b} Experimentation with blends of P3HT and our acceptors showed that 1,2-dichlorobenzene (DCB) had the appropriate combination of solvating power and high boiling point to yield an improved film morphology – likely due to its ability to “solvent anneal” both P3HT and acene-based materials.^{1,21}

Solar cells were fabricated on cleaned, pre-patterned ITO coated glass substrates coated with PEDOT:PSS. Semiconductor layers were deposited by spin-coating of 20 mg ml⁻¹ solutions in a nitrogen-filled glovebox. Finally, 4 Å of CsF and 400 Å of Al were thermally evaporated under high vacuum to form the

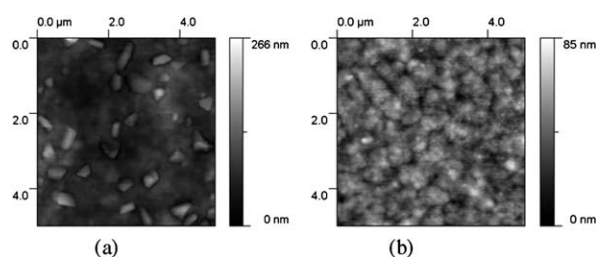


Fig. 4 Atomic force microscopy (AFM) images of 1/P3HT active layers spin-coated from (a) toluene (b) toluene with DCB.

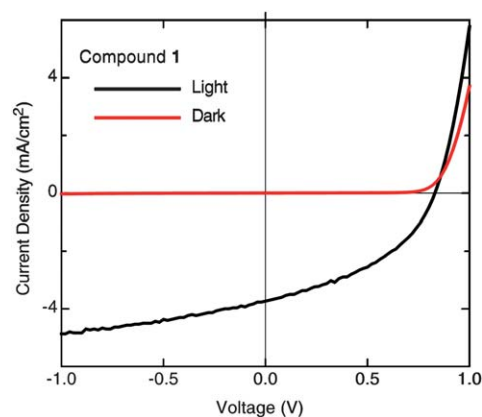


Fig. 5 Current–voltage curve for P3HT/pentacene **1** OPV.

cathode for the devices. Solar cell current–voltage (I – V) curves were measured in the dark and under AM 1.5 100 mW cm⁻² illumination.

A series of comparative studies showed that a P3HT/pentacene blend (1 : 1 ratio by weight) spin-cast from a toluene/DCB solvent mixture (10 : 3 ratio by volume) yielded the highest performing devices. No thermal annealing was performed on the finished devices, since this was typically found to degrade device performance by increasing the domain size of the pentacene acceptor. Clear morphological changes were observed by AFM as the proportion of DCB was increased (Fig. 4), leading to suppression of large crystal formation in one of the semiconductor components and a more uniform grain size. From toluene-cast films, large, coarse crystalline-looking features can be seen, yielding an rms roughness of 22.0 nm (Fig. 4a), whereas the film cast from a toluene/DCB mixture (Fig. 4b) possesses finer features, with a significantly lower film rms (9.1 nm), suggesting more intimate contact between the donor and acceptor phases. Under these conditions, the device performance of cyanopentacene **1** was improved to yield a V_{oc} of 0.84 V, J_{sc} of 3.72 mA cm⁻², FF of 0.41, and a PCE of 1.29% – a representative current–voltage plot is shown in Fig. 5. We note that PCBM-based devices prepared side-by-side with the pentacene devices routinely exhibited PCE of 3.5%.

The other pentacene derivatives shown in Fig. 1 were studied using the optimized fabrication procedure described above, and their device performance is presented in Table 2. All of the

Table 2 Device performance of pentacenes **1–11**

Cpd.	V_{oc}/V	$J_{sc}/\text{mA cm}^{-2}$	FF	PCE (%)
1	0.84 ± 0.01	3.56 ± 0.17	0.42 ± 0.02	1.27 ± 0.03
2	0.79 ± 0.01	0.24 ± 0.02	0.39 ± 0.01	0.08 ± 0.01
3	0.59 ± 0.02	0.54 ± 0.04	0.32 ± 0.02	0.10 ± 0.01
4	0.70 ± 0.01	1.86 ± 0.07	0.32 ± 0.01	0.41 ± 0.02
5	0.67 ± 0.01	2.07 ± 0.22	0.33 ± 0.01	0.46 ± 0.05
6	0.56 ± 0.03	0.27 ± 0.03	0.32 ± 0.01	0.05 ± 0.01
7	0.63 ± 0.03	1.30 ± 0.22	0.29 ± 0.02	0.24 ± 0.04
8	0.64 ± 0.01	0.49 ± 0.03	0.28 ± 0.02	0.09 ± 0.01
9	0.86 ± 0.01	1.05 ± 0.07	0.39 ± 0.02	0.35 ± 0.03
10	0.70 ± 0.01	0.94 ± 0.02	0.37 ± 0.01	0.24 ± 0.01
11	0.79 ± 0.01	0.24 ± 0.02	0.39 ± 0.01	0.08 ± 0.01

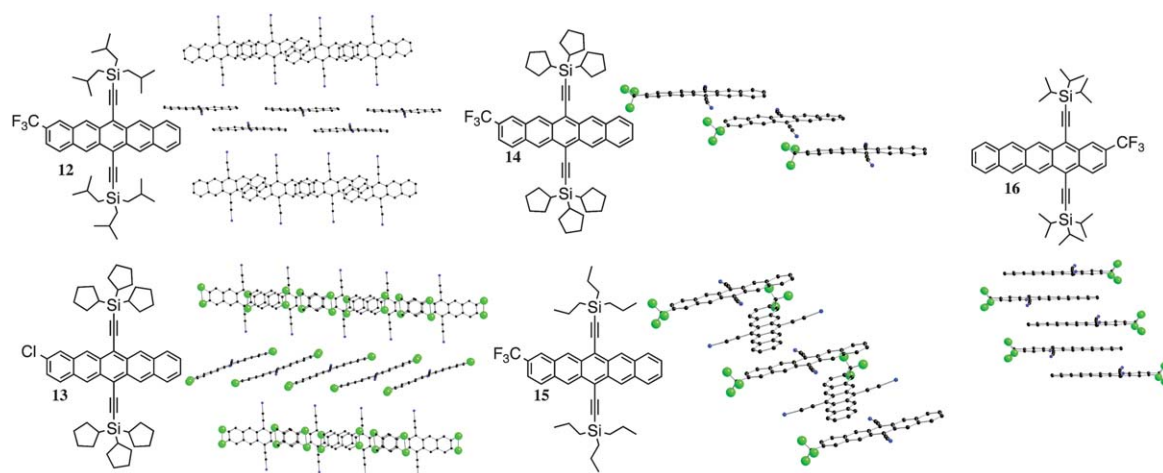


Fig. 6 Structure and crystal packing for pentacenes 12–16. Trialkylsilyl groups hidden for clarity.

materials listed in Fig. 1 yielded working OPVs when blended with P3HT, and nearly all devices show higher V_{oc} than typical P3HT:PCBM cells ($V_{oc} \sim 0.6$ V). A number of arguments have been presented in the literature to describe the impact of material parameters on device V_{oc} , one of the most widely accepted involving the relationship between the donor HOMO and acceptor LUMO.²² Thus for example, TIPS pentacene (**11**), a known p-type semiconductor in OTFTs,²³ has the highest lying LUMO of all the materials tested and correspondingly exhibited one of the highest V_{oc} . However, there is also an observed relationship between V_{oc} and film morphology,²⁴ which may relate to the observed impact of the substitution pattern on the V_{oc} of the solar cells. All derivatives substituted on the 1-position of the acene (**2**, **3**, **6**) showed demonstrably lower V_{oc} than derivatives containing the same electron-withdrawing group at the 2-position (**1**, **4**, **8**). The magnitude of this difference (in all cases > 0.05 V) is significantly greater than would be estimated from the differences in LUMO energies (on the order of 0.0–0.04 eV). Contributing to this phenomenon may be the very different crystallinity of the 1-substituted *vs.* the 2-substituted derivatives – as mentioned previously, *none* of the 1-substituted derivatives presented here yielded crystals suitable even for crystallographic analysis.

Structural optimization for improved device current

In general, the materials whose π -stacking motif approach 1-D π -stacking exhibit higher J_{sc} and hence higher PCE, consistent with our previous observations.¹⁵ In our previous study, we found that the derivative adopting a “sandwich herringbone”

crystal packing arrangement (*e.g.* **1**) yielded the highest J_{sc} in blends with P3HT. The silylthyne route to acene functionalization allows facile tuning of crystal packing by simple changes to the silane, and a number of derivatives were screened for this desirable motif. While the carboxymethyl derivative could not be altered to yield the desired crystal packing, both the trifluoromethyl derivative **12** (requiring the tri-*iso*-butylsilyl substituent) and the chloro derivative **13** (requiring a tricyclopentylsilyl substituent) did yield appropriate motifs (Fig. 6). For **12**, extensive disorder in the *iso*-butyl groups (omitted in Fig. 6) precluded refinement of the structural model, but the sandwich herringbone motif is quite apparent from the data. For **13**, four-fold disorder in the position of the single chlorine substituent (apparent in the structure shown in Fig. 6) also prevented detailed structural refinement – but the packing motif is quite clear. Unlike compound **12**'s sandwich herringbone motif, compound **13** adopts an unusual form of the 1-D slipped-stack, where adjacent stacks interact in an edge-to-face, rather than coplanar orientation. We refer to this motif as “sandwich slipped-stack”. It is worth noting that the trifluoromethyl derivative also yielded materials with crystal motifs not previously screened for OPV performance; a simple 1-D “slipped-stack” motif¹⁸ (**14**, tricyclopentylsilyl substituent) and an unusual “cruciform” version of this motif, where alternate pentacene units are rotated by approximately 90° relative to their neighbors in the stack (**15**, tri-*n*-propylsilyl derivative). The apparent beneficial nature of materials with 1-D π -stacking motifs also led us to synthesize “offset” pentacene derivative **16**, which we knew from prior experience would yield essentially columnar π -stacked arrays. Following the procedure optimized for derivative **1**, BHJ solar cells were made from blends of **12–16** with P3HT. The device parameters for these new cells are listed in Table 3.

Yet again, we see that materials adopting a sandwich-type crystal packing arrangement (**12**, **13**) yield the highest device currents and fill-factors (J - V plots for **12** and **13** are presented in the ESI†). The requirement of a strongly one-dimensional packing motif for best performance is further supported by the reasonably good performance of derivative **14** which, although not adopting a sandwich-type motif, still packs in a 1-D slipped-stack arrangement with a similarly insulated π -stacking channel.

Table 3 Device performance of pentacene acceptors 12–16

Cpd.	V_{oc}/V	$J_{sc}/mA\ cm^{-2}$	FF	PCE (%)
12	0.80 ± 0.02	3.17 ± 0.03	0.50 ± 0.01	1.26 ± 0.01
13	0.95 ± 0.02	2.44 ± 0.13	0.43 ± 0.01	1.00 ± 0.08
14	0.78 ± 0.01	3.23 ± 0.06	0.33 ± 0.01	0.83 ± 0.03
15	0.62 ± 0.01	1.05 ± 0.06	0.27 ± 0.01	0.18 ± 0.01
16	0.32 ± 0.01	0.40 ± 0.02	0.40 ± 0.02	0.05 ± 0.01

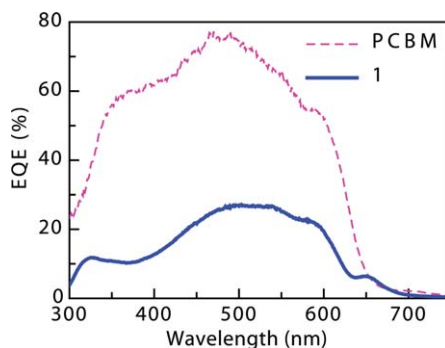


Fig. 7 EQE spectra of BHI solar cells based on 1:P3HT (solid) and PCBM:P3HT (dashed).

Compounds **15** and **16**, which adopt 1-D *columnar* π -stacking arrangements, showed device performance roughly an order of magnitude worse than derivatives adopting other 1-D π -stacking motifs. The particularly poor performance of **16** may also be explained by the lower stability of this material – there are no substituents protecting the relatively reactive 6,13 positions of the pentacene backbone.

Further device characterization

To further investigate OPV performance of these acceptors, the EQE spectrum of derivative **1** in a blend with P3HT was acquired (Fig. 7). The peak EQE is above 25% at around 500 nm for this device, corresponding to the peak absorption of P3HT. The smaller peaks at around 330 nm and 650 nm correspond to the absorption peaks of pentacene **1**, showing that it too is contributing to the generation of photocurrent outside the absorption window of P3HT, effectively extending the spectral response of the P3HT-based solar cell.

Finally, as a preliminary study of the stability of these new materials, their operational performance was characterized in air alongside that of a traditional P3HT/PCBM device fabricated at the same time. As shown in Fig. 8, the device lifetime of pentacene-based materials was comparable to that of the simultaneously measured PCBM-based device.

Conclusion

We have demonstrated that several silylthyne-substituted pentacene derivatives successfully serve as effective acceptors in

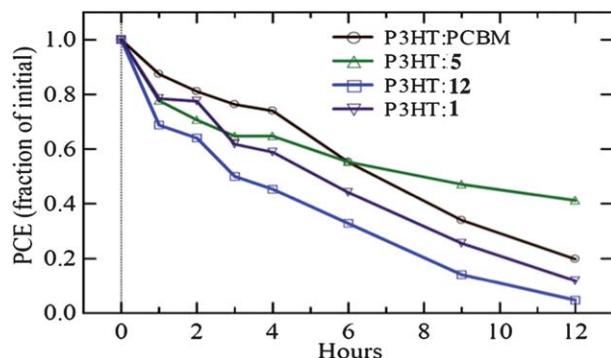


Fig. 8 Comparison of device lifetime of pentacene-based solar cells vs. PCBM-based devices.

P3HT-based BHI solar cells. Using an improved fabrication procedure that exploits solvent mixtures to yield better film morphology, we found that both the nature and position of electron-withdrawing groups substituted onto the pentacene chromophore impact the device V_{oc} . Both inductive and resonance electron-withdrawing groups substituted at the pentacene 2-position led to devices with voltages higher than typically observed with PCBM acceptor, with cyano, trifluoromethyl and chloro substituents yielding the best performance. After determining the aromatic ring substituents yielding the best voltage, optimization of the acceptor crystal packing by changing the alkyl groups on the silyl substituent led to improvements in device current. We found that a particular crystal packing arrangement – the “sandwich herringbone” motif – consistently yielded the best photocurrents. Studies to understand the particular reason for the improved photocurrent are currently underway. Our experiments have yielded three new acceptors all with power conversion efficiency >1.0%, with the best derivative, cyano-substituted **1**, exhibiting a PCE approaching 1.3%. These results are among the best reported for non-fullerene small-molecule acceptors for polymer BHI solar cells. The wide array of pentacene derivatives that yield efficient solar cells, the ease with which new derivatives can be prepared, and the structure/function relationships that are beginning to emerge from this study make these pentacenes a versatile platform for the development of new OPV acceptors.

Acknowledgements

J. E. A. and G. G. M. thank the Office of Naval Research for support of this research effort. Y. F. L. acknowledges a research fellowship from A*STAR (Singapore). B. P. acknowledges the National Science Foundation for support.

Notes and references

- G. Yu, J. Gao, J. C. Hummelen, F. Wudl and A. J. Heeger, *Science*, 1995, **270**, 1789.
- G. Li, V. Shrotriya, J. Huang, Y. Yao, T. Moriarty, K. Emery and Y. Yang, *Nat. Mater.*, 2005, **4**, 864; W. Ma, C. Yang, X. Gong, L. Lee and A. J. Heeger, *Adv. Mater.*, 2005, **17**, 1617; B. C. Thompson and J. M. J. Fréchet, *Angew. Chem., Int. Ed.*, 2008, **47**, 58; F. G. Brunetti, R. Kumar and F. Wudl, *J. Mater. Chem.*, 2010, **20**, 2934; W. Cai, X. Gong and Y. Cao, *Sol. Energy Mater. Sol. Cells*, 2010, **94**, 114.
- C. Piliago, T. W. Holcombe, J. D. Douglas, C. H. Woo, P. M. Beaujuge and J. M. J. Fréchet, *J. Am. Chem. Soc.*, 2010, **132**,

- 7595; Y. Zou, A. Najari, P. Berrouard, B. Beaupré, B. R. Aïch, Y. Tao and M. Leclerc, *J. Am. Chem. Soc.*, 2010, **132**, 5330; Y. Liang, Y. Wu, D. Feng, S.-T. Tsai, H.-J. Son, G. Li and L. Yu, *J. Am. Chem. Soc.*, 2009, **131**, 56; J. Chen and Y. Cao, *Acc. Chem. Res.*, 2009, **42**, 1709.
- 4 Y. Yao, J. Hou, Z. Xu, G. Li and Y. Yang, *Adv. Funct. Mater.*, 2008, **18**, 1; J. K. Lee, W. L. Ma, C. J. Brabec, J. Yuen, J. S. Moon, J. Y. Kim, K. Lee, G. C. Bazan and A. J. Heeger, *J. Am. Chem. Soc.*, 2008, **130**, 3619; L.-M. Chen, Z. Xu, Z. Hong and Y. Yang, *J. Mater. Chem.*, 2010, **20**, 2575.
- 5 H. Y. Chen, J. H. Hou, S. Q. Zhang, Y. Y. Liang, G. W. Yang, Y. Yang, L. Yu, Y. Wu and G. Li, *Nat. Photonics*, 2009, **3**, 649.
- 6 J. J. Dittmer, E. A. Marseglia and R. H. Friend, *Adv. Mater.*, 2000, **12**, 1270.
- 7 T. Kietzke, H.-H. Horhold and D. Neher, *Chem. Mater.*, 2005, **17**, 6532; X. Zhan, Z. Tan, B. Domercq, Z. An, X. Zhang, S. Barlow, Y. Li, D. Zhu, B. Kippelen and S. R. Marder, *J. Am. Chem. Soc.*, 2007, **129**, 7246; T. W. Holcombe, C. Woo, D. F. J. Kavulak, B. C. Thompson and J. M. J. Fréchet, *J. Am. Chem. Soc.*, 2009, **131**, 14160.
- 8 S. Rajaram, P. B. Armstrong, B. J. Kim and J. M. J. Fréchet, *Chem. Mater.*, 2009, **21**, 1775.
- 9 Z. E. Ooi, T. L. Tam, R. Y. C. Shin, Z. Chen, T. Kietzke, A. Sellinger, M. Baumgarten, K. Mullen and J. C. deMello, *J. Mater. Chem.*, 2008, **18**, 4619; R. Y. C. Shin, T. Kietzke, S. Sudhakar, A. Dodabalapur, Z.-K. Chen and A. Sellinger, *Chem. Mater.*, 2007, **19**, 1892; C. H. Woo, T. W. Holcombe, D. A. Unruh, A. Sellinger and J. M. J. Fréchet, *Chem. Mater.*, 2010, **22**, 1673; R. Y. C. Shin, P. Sonar, P. S. Siew, Z.-K. Chen and A. Sellinger, *J. Org. Chem.*, 2009, **74**, 3293.
- 10 P. Sonar, G.-M. Ng, T. T. Lin, A. Dodabalapur and Z.-K. Chen, *J. Mater. Chem.*, 2010, **20**, 3626.
- 11 Y. Zhou, J. Pei, Q. Dong, X. Sun, Y. Liu and W. Tian, *J. Phys. Chem. C*, 2009, **113**, 7882.
- 12 F. Brunetti, X. Gong, A. J. Heeger and F. Wudl, *Angew. Chem., Int. Ed.*, 2010, **49**, 532.
- 13 J. E. Anthony, *Angew. Chem., Int. Ed.*, 2008, **47**, 452.
- 14 Y. Sakamoto, T. Suzuki, M. Kobayashi, Y. Gao, Y. Fukai, Y. Inoue, F. Sato and S. Tokito, *J. Am. Chem. Soc.*, 2004, **126**, 8138.
- 15 Y.-F. Lim, Y. Shu, S. R. Parkin, J. E. Anthony and G. G. Malliaras, *J. Mater. Chem.*, 2009, **19**, 3049.
- 16 B. M. Medina, J. E. Anthony and J. Gierschner, *ChemPhysChem*, 2008, **9**, 1519.
- 17 I. Seguy, P. Jolinat, P. Destruel, R. Mamy, H. Allouchi, C. Courseille, M. Cotrait and H. Mock, *ChemPhysChem*, 2001, **2**, 448.
- 18 J. E. Anthony, D. L. Eaton and S. R. Parkin, *Org. Lett.*, 2002, **4**, 15.
- 19 J. E. Anthony, J. S. Brooks, D. L. Eaton and S. R. Parkin, *J. Am. Chem. Soc.*, 2001, **123**, 9482.
- 20 X. Yang, J. Loos, S. C. Veenstra, W. J. H. Verhees, M. M. Wienk, J. M. Kroon, M. A. J. Michels and R. A. J. Janssen, *Nano Lett.*, 2005, **5**, 579.
- 21 M. T. Lloyd, A. C. Mayer, S. Subramanian, D. A. Mourey, D. J. Herman, A. V. Bapat, J. E. Anthony and G. G. Malliaras, *J. Am. Chem. Soc.*, 2007, **129**, 9144.
- 22 C. J. Brabec, A. Cravino, D. Meissner, N. S. Sariciftci, T. Fromherz, M. T. Rispens, L. Sanchez and J. C. Hummelen, *Adv. Funct. Mater.*, 2001, **11**, 374; C. J. Brabec, A. Cravino, D. Meissner, N. S. Sariciftci, M. T. Rispens, L. Sanchez, J. C. Hummelen and T. Fromherz, *Thin Solid Films*, 2002, **403–404**, 368.
- 23 S. K. Park, T. N. Jackson, J. E. Anthony and D. Mourey, *Appl. Phys. Lett.*, 2007, **91**, 063514.
- 24 M. C. Scharber, D. Mühlbacher, M. Koppe, P. Denk, C. Waldauf, A. J. Heeger and C. J. Brabec, *Adv. Mater.*, 2006, **18**, 789.